THE JOURNAL OF PHYSICAL CHEMISTRY B

Article

pubs.acs.org/JPCB

Ion Transport Effects in a Solid Polymer Electrolyte Due to Salt Substitution and Addition Using an Ionic Liquid

Johannes Kösters,[†] Monika Schönhoff,[‡] and Nicolaas A. Stolwijk*,[†]

[†]Institut für Materialphysik, University of Münster, Wilhelm-Klemm-Str. 10, 48149 Münster, Germany

[‡]Institut für Physikalische Chemie, University of Münster, Corrensstr. 28/30, 48149 Münster, Germany

ABSTRACT: We investigated mass and charge transport in amorphous salt-in-poly(ethylene oxide) (PEO) electrolytes with NaI and/or the ionic liquid (IL) EMImTFSI (1-ethyl-3-methylimizadolium bis(trifluoromethylsulfonyl)imide) as salt component. Combining the results of ion conductivity, pulsed field gradient nuclear magnetic resonance, and radiotracer diffusion measurements, it is found that over wide temperature ranges both the cation and anion diffusion coefficients and the charge diffusivity are distinctly larger in PEO_{20}EMImTFSI than in PEO_{20}NaI complexes, where the monomer-to-salt mole ratio equals 20. In the mixed-salt complexes $PEO_{20}NaI_1EMImTFSI_1$ and $PEO_{20}NaI_{0.5}EMImTFSI_{0.5}$, we observe a slowing down of the IL ions EMIm and TFSI along with a diffusivity enhancement of the I anion compared to the single-salt base complexes. For the cation Na, a diffusivity increase is only effected by IL substitution, but because of the concomitant decrease of the Na concentration, it does not predict more effective charge transfer in a battery cell configuration.

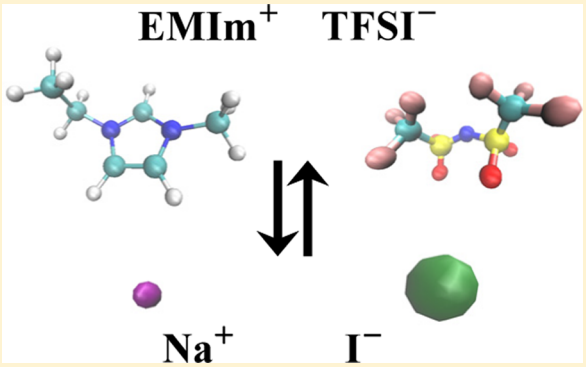

1. INTRODUCTION

Solid-like polymer electrolytes (SPEs), polymeric membranes with dissolved salts, have been investigated for almost four decades because of their promising applications, e.g., in lithium batteries. The advantages of SPEs include low flammability, chemical stability, and mechanical flexibility thereby outperforming organic−liquid electrolytes in terms of safety and leakage problems. In particular, poly(ethylene oxide) (PEO) has proven to be a suitable SPE matrix owing to its good solvation properties for alkali metal salts. However, a drawback of solvent-free PEO-based electrolytes is their limited ionic conductivity, also at elevated temperatures just above the PEO melting temperature. Even more severe is the fact that in these classical dry systems the technologically relevant cations (Li and Na) are much less mobile than the anions.

To overcome these disadvantages, in recent years, the addition of room-temperature ionic liquids (ILs) to conventional SPEs was proposed.[1,2] ILs are a special type of molten salts with the melting point below or at least close to room temperature (<100 °C). They usually consist of a bulky organic cation and an inorganic anion. Outstanding IL properties are a negligible vapor pressure and a high electrochemical stability window. In fact, several studies by S. Passerini and co-workers reported the improvement of battery performance due to the addition of IL to the solvent-free PEO-based electrolyte.[3,4] A similar investigation confirmed the distinct conductivity increase of such an electrolyte by its blending with different ILs.[5] It should be noted, however, that a mere enhancement of the conductivity seems less relevant technologically since it may be due to the IL cation and/or the anion and thus not necessarily imply a higher mobility of the alkali metal cation (e.g., Li).

In a very recent study by Joost et al.,[6] the effect of IL addition on PEO−LiTFSI electrolytes was comprehensively investigated by using a variety of experimental techniques including pulsed field gradient nuclear magnetic resonance (PFG-NMR) to measure ion-specific diffusion coefficients. A major result of this work was the observed enhancement of the Li diffusivity upon IL addition for the composition EO/Li = 20:1 (i.e., by about 50% at 50 °C). However, no increase of the Li diffusivity was found for the more salt-concentrated 10:1 composition. Moreover, the temperatures investigated by Joost et al. cover the narrow range from 20 to 50 °C in which the degree of PEO crystallization may crucially depend on the added amount of IL, as indicated by their DSC measurements. Therefore, the results of that study heavily bear on the morphological/structural effects of the IL admixture.

The present work is a basic study on ion-transport and ion-association effects in PEO-based electrolytes with IL and/or alkali metal salt. The study is carried out on the $PEO_{20}NaI_xEMImTFSI_y$ electrolyte system with x, y = 0, 0.5, or 1, including the ternary, mixed-salt complexes $PEO_{20}NaI_{0.5}EMImTFSI_{0.5}$ and $PEO_{20}NaI_1EMImTFSI_1$ and the binary, single-salt complexes PEO_{20}NaI and PEO_{20}EMImTFSI. Our particular interest concerns the question whether the transport properties of the battery-

Received: November 23, 2012
Revised: January 22, 2013
Published: January 30, 2013

relevant alkali metal ion (Na) can be improved either by the partial substitution of NaI with the ionic liquid EMImTFSI or by the addition of EMImTFSI to the binary PEO−NaI electrolyte.

The experimental data cover a wide range of elevated temperatures from 70 °C to at least 170 °C), where the electrolytes are all fully amorphous, irrespective of the amount of dissolved IL or salt. The choice of systems and T-range is motivated by the following considerations: (i) In contrast to the earlier studies cited above, the present system involves besides two different cations (Na, EMIm) also two different anions (I, TFSI). This enables us to investigate the effects on anion diffusion in more detail. (ii) Not only the two cations but also the two anions greatly differ in size and shape. (iii) Previously acquired data on the PEO−NaI system[7] and the available expertise on diffusion experiments with the four pertinent ions formed a solid base for obtaining reliable results. (iv) Temperatures above the melting temperature of PEO (65 °C) avoid complications due to crystallization and phase separation, which may lead to strong variations in morphology. (v) The chosen cations and anions are relevant to application-oriented fields such as, e.g., sodium batteries (Na, TFSI) and dye-sensitized solar cells (EMIm, I).

Our main experimental techniques comprise electrochemical impedance spectroscopy (EIS), PFG-NMR, and radiotracer diffusion (RTD), which enable us to measure the ionic conductivity (or charge diffusivity), the self-diffusivity of EMIm and TFSI, and the tracer-diffusivity of ^{22}Na and ^{125}I, respectively. In this manner, we are able to monitor effects on mass and charge transport for both IL/NaI substitution and IL or NaI addition. The influence of the glass transition temperature and the extent of ion association are also assessed in this article. The results of this fundamental investigation may help future developments in electrolyte technology.

2. EXPERIMENTAL SECTION

2.1. Materials and Preparation. The base materials were PEO with a molecular weight of 8×10^6 g/mol and a purity of 98.4 wt %[8] (Aldrich), EMImTFSI (391.3 g/mol, 99.9 wt %, Solvionic), , and NaI (149.9 g/mol, >99 wt %, Grüssing). All substances were vacuum-dried before use. For the ionic liquid EMImTFSI, the water content was determined to be in the 100 ppm range by Karl Fischer titration. For the preparation of the binary and ternary polymer electrolytes, the same methods were used as described in earlier publications by our group.[9,10] Great care was taken to remove traces of water and solvent (dry acetonitrile) and to avoid contact with ambient atmosphere. In (PFG-)NMR analysis, no ^{1}H resonance attributable to water could be detected. Considering that all preparation steps were either carried out in a nitrogen-filled glovebox (H_2O < 1 ppm) or under dynamic vacuum, the water contamination of the SPEs is assumed to be at the 10 ppm level or below.

2.2. Electrolyte Characterization. The mass density of the electrolytes was determined by hydrostatic weighing in dodecane and air, taking single-crystal silicon as reference material. The density enters the calculation of the salt concentration per unit volume. Phase behavior was examined by differential scanning calorimetry (DSC) at different heating and cooling rates using Perkin-Elmer DSC-7 and DSC-9 devices. Within the temperature range of the conductivity and diffusion measurements (see below), no indications for salt or IL precipitation were found. T_g values determined after ex situ quenching in a dewar with liquid nitrogen (1st heating cycle) and in situ quenching in the calorimeter (2nd heating cycle) were mutually consistent.

2.3. Impedance Spectroscopy. The ionic conductivity was measured by impedance spectroscopy in the frequency range from 5 Hz to 13 MHz using an HP Agilent 4192A LF impedance analyzer.[11] The reliability of the data was ensured by using at least two different samples for each composition and by running multiple heating and cooling cycles for each sample. As ionic conduction mainly takes place in the amorphous phase of the electrolytes, the data covered the widest possible temperature range of this phase. In practice, this range extended roughly from 50 to 200 °C. The consistency of the results over measurement periods of several days for each sample points to a sufficient stability of the electrolytes in the T-range of interest.

2.4. Pulsed-Field-Gradient Nuclear Magnetic Resonance. Diffusion coefficients of different ionic species were measured on a 400 MHz FT-NMR spectrometer (Bruker, Avance) employing a probe head (Bruker, DIFF 30) with RF-selective inserts for the respective nuclei and providing a magnetic field gradient strength of up to 12 T/m. The stimulated echo was employed with a variation of the gradient strength, g.

The diffusivity of the organic cation D^*_{EMIm} was obtained from ^{1}H nuclei of EMIm. Similarly, D^*_{TFSI} was monitored using the ^{19}F resonance of the TFSI anion. The intensity I of the echo signal decreases with increasing g according to[12]

$$I = I_0 \exp(-k_{PFG} D^*) \tag{1}$$

with

$$k_{PFG} = \gamma^2 g^2 \delta^2 \left(\Delta - \frac{\delta}{3}\right) \tag{2}$$

Here, I_0 denotes the zero-gradient intensity, D^* is the diffusion coefficient, γ is the gyromagnetic ratio, δ is the duration of the gradient pulse, and Δ is the observation time for the mean square displacement.

Of the six different EMIm-related ^{1}H-resonances, there are two resonances that interfere mutually and two other ones that overlap with the strong, hardly attenuated PEO signal. Thus, each of the distinguishable three peaks yields a value for D^*_{EMIm} at a selected temperature. The data presented below are the corresponding mean values and further characterized by a standard deviation of about 10%. By contrast, the D^*_{TFSI} data arise from the coincident resonances of six equivalent ^{19}F nuclei.

2.5. Radiotracer Diffusion. The diffusivities of Na and I were measured by the RTD method, which is described in detail elsewhere.[13] The radionuclides ^{22}Na and ^{125}I with half-lives of 2.6 years and 60 days, respectively, were used as tracers. After placing a radioactive polymer-electrolyte source film on top of a sample and subsequent isothermal annealing in an oil bath, the sample was sectioned with a rotary microtome at a suitable freezing temperature. In many cases, both ^{22}Na and ^{125}I were contained in the source film and thus diffused simultaneously into the sample. Tracer depth profiles were obtained by counting the tracer-specific radiation in each section. D^*_{Na} and D^*_I were determined by fitting the measured penetration profiles with the appropriate solution of Fick's second law[13]

$$c(x, t) = \frac{1}{2} c_0 \left[\operatorname{erfc}\left(\frac{x}{2\sqrt{D^* t}}\right) + \operatorname{erfc}\left(\frac{x + 2h}{2\sqrt{D^* t}}\right)\right] \tag{3}$$

dx.doi.org/10.1021/jp311563h | J. Phys. Chem. B 2013, 117, 2527−2534

Here, c_0 denotes the tracer concentration (activity) of the source layer of width h, whereas $c(x,t)$ is the corresponding value at depth x after a diffusion treatment characterized by the diffusivity D^* and the time t. For extremely low and high values of $h/(D^*t)^{1/2}$, eq 3 converges to the Gaussian and complementary error function, respectively. It should be emphasized that the concentrations of ^{22}Na and ^{125}I are always very low fractions of the total sodium and iodine content, so that their diffusion does *not* involve changes in composition. In contrast to PFG-NMR, the RTD technique is destructive, so that each measurement requires a new sample.

3. RESULTS AND EVALUATION

3.1. Glass Transition and Conductivity. The $PEO_{20}NaI_xEMImTFSI_y$ electrolytes investigated in this work will be denoted henceforward by the concise form $20/x/y$, where x and y equal 0, 0.5, or 1. Thus, 20/0/1 refers to the binary $PEO_{20}EMImTFSI$ complex. The general characteristics of the electrolytes are compiled in Table 1. These include the mass density ρ, the glass transition temperature T_g, and the total salt concentration C_s. In the mixed-salt complexes 20/0.5/0.5 and 20/1/1, the separate IL and NaI concentrations are equal to $C_s/2$.

Table 1. Mass Density ρ, Glass Transition Temperature T_g, and Total Salt Concentration C_s (Number Density and in Units of mol/L) of $PEO_{20}NaI_xEMImTFSI_y$ Complexes (20/x/y); Estimated Experimental Errors: 2.0% (ρ), 2 °C (T_g), and 2.5% (C_s)

complex	ρ (gcm^{-3})	T_g (°C)	C_s (cm^{-3})	C_s (mol/L)
20/1/0	1.33	−12.3	7.76×10^{20}	1.29
20/0/1	1.29	−63.3	6.12×10^{20}	1.02
20/0.5/0.5	1.28	−37.6	6.70×10^{20}	1.11
20/1/1	1.34	−43.2	1.13×10^{21}	1.88

It is remarkable that ρ does not vary much with composition. However, T_g decreases with increasing IL content for the three first listed complexes with a PEO/total-salt ratio of 20:1. Interestingly, $T_g = -37.6°$ for the 20/0.5/0.5 complex coincides within experimental error (±2 °C) with the mean T_g value of the two binary complexes. The more concentrated mixed-salt electrolyte 20/1/1 undergoes the glass transition at a slightly lower temperature, i.e., −43.2 °C.

Figure 1 shows the temperature dependence of the DC conductivity σ for the two mixed-salt complexes 20/0.5/0.5 and 20/1/1. The temperature range extends from about 45 to 200 °C within the fully amorphous phase of the complexes. The experimental data are fitted by the Vogel−Tammann−Fulcher (VTF) equation

$$\sigma(T) = \sigma_0 \exp\left(-\frac{B_\sigma}{T - T_{\sigma 0}}\right) \quad (4)$$

Here, σ_0 denotes a pre-exponential factor, T is temperature, $T_{\sigma 0}$ is a reference temperature at which the ionic mobility vanishes, and B_σ is an activation temperature or pseudo activation energy. It should be mentioned, however, that no physical meaning is attributed to the parameter values obtained by the fitting with eq 4; they only serve as a phenomenological description (see the solid lines in Figure 1). It is seen that the 20/1/1 complex has a higher conductivity than the 20/0.5/0.5 one. The difference between both data sets weakly varies with temperature and roughly corresponds to a factor of 2, which complies with the difference in total salt content.

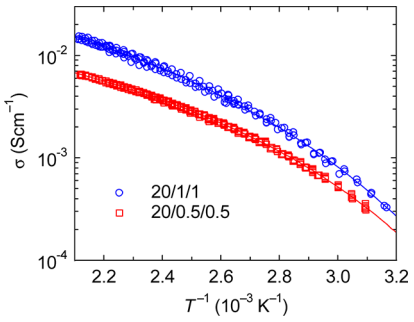

Figure 1. DC conductivity of $PEO_{20}NaI_{0.5}EMImTFSI_{0.5}$ and $PEO_{20}NaI_1EMImTFSI_1$ electrolytes as a function of inverse temperature. The solid lines are fits based on the VTF expression (cf. eq 4).

The Nernst−Einstein equation enables us to convert the conductivity into a diffusion coefficient, i.e., the charge diffusivity D_σ. In this work, we use the specific form

$$D_\sigma = \frac{k_B T}{C_s e^2}\sigma \quad (5)$$

where k_B denotes the Boltzmann constant and e is elementary charge. It is noteworthy that eq 5 contains the known total salt concentration C_s (number density of molecules) including NaI and IL instead of the a priori unknown concentration of free (dissociated) ions. This allows us to treat D_σ as an experimental quantity that can be directly compared with the other measured diffusion coefficients D^*_{Na}, D^*_I, D^*_{EMIm}, and D^*_{TFSI}, as demonstrated in Figure 4 to be discussed later on.[14] It should be emphasized, that information on the extent of ion pairing is contained in the collectivity of the ionic diffusion coefficients including the charge diffusivity (see below). The C_s values of the investigated electrolytes are compiled in Table 1 together with other relevant characteristics.

3.2. Ionic Diffusion Data. Figure 2 displays for the 20/0/1 complex the normalized intensity of the PFG-NMR signal associated with the EMIm cation as a function of magnetic field strength (contained in k_{PFG}) at different temperatures. Specifically, the data of the largest ^{1}H peak associated with the highest resonance frequency are plotted. According to eqs 1 and 2, the T-dependence of the EMIm diffusivity is reflected by

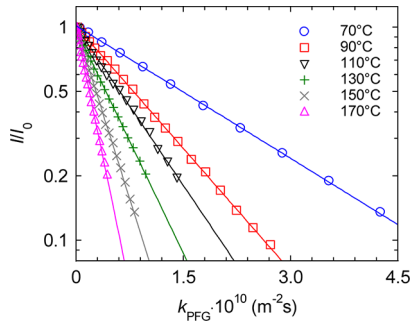

Figure 2. Decay of the normalized ^{1}H PFG-NMR signal intensity I/I_0 in $PEO_{20}EMImTFSI$ for various temperatures as a function of the magnetic field gradient contained in the parameter. The cation diffusivity D^*_{cat} is calculated from the slope of the straight-line fits according to eqs 1 and 2.

dx.doi.org/10.1021/jp311563h | J. Phys. Chem. B 2013, 117, 2527−2534

the differences in slope of the straight lines fitted to the experimental data (symbols). The data originating from different EMIm-related ^{1}H peaks were found to be mutually consistent in all IL-containing systems. Similarly good signals were obtained for the ^{19}F resonance monitoring TFSI diffusion. The resulting values of D^{*}_{EMIm} and D^{*}_{TFSI} are plotted in Figure 4 as up-triangles and circles, respectively.

Figure 3 shows two typical radiotracer depth profiles in 20/1/1, one for ^{22}Na, the other for ^{125}I, to illustrate the original

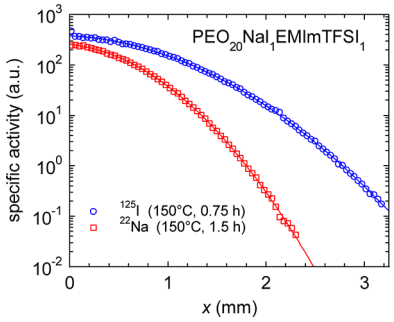

Figure 3. Depth profiles of the radiotracers ^{22}Na and ^{125}I in $PEO_{20}NaI_1EMImTFSI_1$ measured after diffusion treatments given by the indicated temperature and times.

results obtained by the radiotracer technique. The profiles extend over more than 3 orders of magnitude in specific activity and over more than 2 mm in penetration depth. The solid lines are least-squares fits based on eq 3 (cf. section 2.5) showing virtual perfect coincidence with the experimental data. The D^{*}_{Na} and D^{*}_{I} data resulting from the RTD measurements are plotted in Figure 4 as down-triangles and squares, respectively.

Figure 4 provides a survey of the diffusivities obtained for the binary (20/0/1 and 20/1/0) and ternary electrolytes (20/0.5/0.5 and 20/1/1) investigated. The solid lines are VTF fits that serve to guide the eye. The corresponding parameter values are compiled in Table 2. It is seen that in the pure PEO−IL

Table 2. Parameter Values Describing the Fits of the Diffusivity Data in Figures 4−6 with the VTF Equation $D = D_0 \exp(B/(T - T_0))$ (Solid Lines)

complex	diffusivity	D_0 (cm^2 s^{-1})	B (K)	T_0 (K)
20/1/0	D^{*}_{Na}	1.60×10^{-4}	1560	166.7
	D^{*}_{I}	2.67×10^{-5}	682.5	217.2
	D_σ	1.77×10^{-5}	624.9	226.0
20/0/1	D^{*}_{EMIm}	3.95×10^{-4}	1508	118.6
	D^{*}_{TFSI}	3.95×10^{-4}	1549	124.8
	D_σ	7.13×10^{-6}	636.7	204.9
20/0.5/0.5	D^{*}_{Na}	1.98×10^{-5}	952.6	183.4
	D^{*}_{I}	2.19×10^{-5}	628.3	197.1
	D^{*}_{EMIm}	6.53×10^{-5}	807.8	192.1
	D^{*}_{TFSI}	9.46×10^{-5}	1008	179.1
	D_σ	3.64×10^{-5}	727.3	202.6
20/1/1	D^{*}_{Na}	1.26×10^{-3}	2630	103.8
	D^{*}_{I}	9.23×10^{-5}	928.4	203.0
	D^{*}_{EMIm}	1.99×10^{-4}	1131	180.6
	D^{*}_{TFSI}	1.71×10^{-4}	1199	177.7
	D_σ	6.17×10^{-5}	807.9	202.3

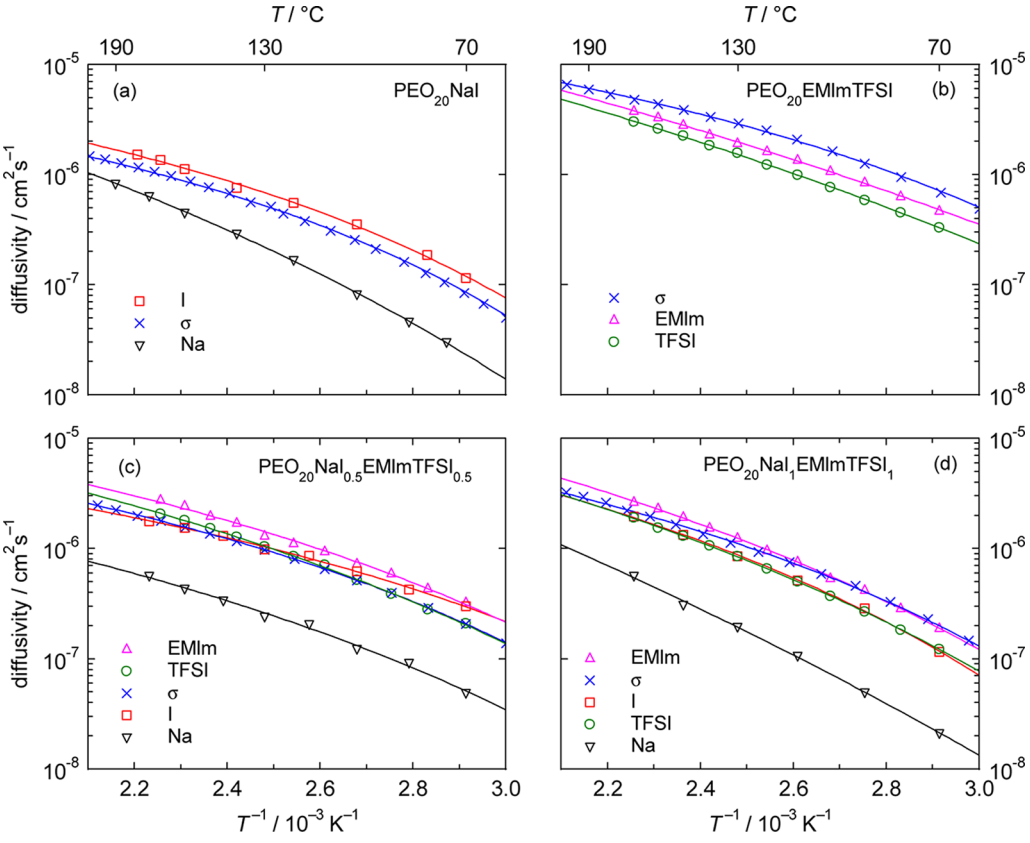

Figure 4. Diffusivity of cations (D^{*}_{Na} and D^{*}_{EMIm}) and anions (D^{*}_{I} and D^{*}_{TFSI}) as a function of inverse temperature compared to the charge diffusivity D_σ in single-salt and mixed-salt $PEO_{20}NaI_xEMImTFSI_y$ (20/x/y) electrolytes: (a) 20/1/0, (b) 20/0/1, (c) 20/0.5/0.5, and (d) 20/1/1 . The solid lines are VTF fits serving to guide the eye.

dx.doi.org/10.1021/jp311563h | J. Phys. Chem. B 2013, 117, 2527−2534

complex (Figure 4b) the ionic and charge diffusion proceed faster than in the pure PEO-NaI complex (Figure 4a) of the same EO/salt ratio. In the corresponding intermixed case (20/0.5/0.5, Figure 4c), four out of five diffusion coefficients are grouped together at intermediate positions with respect to the single-salt complexes; only D^*_{Na} clearly runs below the other data. A similar picture arises for the more concentrated mixed-salt electrolyte (20/1/1, Figure 4d).

3.3. Evaluation of Mass and Charge Transport. A comparison of all D_σ data is given by Figure 5. Both mixed-salt electrolytes fall between the two binary cases. The near D_σ coincidence of 20/0.5/0.5 and 20/1/1 reflects the approximate factor-of-two difference in σ (cf. Figure 1) and the division by C_s in eq 5. The 50% *replacement* of NaI by IL starting from 20/1/0 (lower data) gives rise to an increase of the charge diffusivity by a factor varying from 2 (high T) to 3 (low T). Conversely, a similar substitution of IL in 20/0/1 (upper data) by NaI leads to a drop in D_σ by a factor of 4. From the viewpoint of NaI or IL *addition*, similar changes are observed, as reflected by the 20/1/1 data with regard to the binary terminal complexes. In agreement with common observations, D_σ globally anticorrelates with the glass transition temperature T_g listed in Table 1.

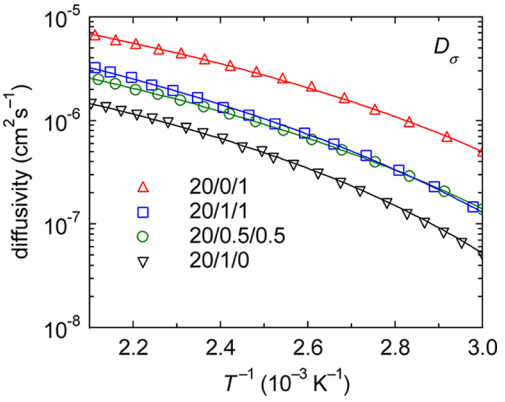

Figure 5. Charge diffusivity D_σ as a function of inverse temperature in single-salt and mixed-salt $PEO_{20}NaI_xEMImTFSI_y$ (20/x/y) electrolytes, as indicated. The solid lines are VTF fits serving to guide the eye.

In Figure 6, the data are sorted according to anion diffusivity ($D^*_{an} = D^*_I$ or D^*_{TFSI}; panels a and b) and cation diffusivity ($D^*_{cat} = D^*_{Na}$ or D^*_{EMIm}; panels c and d). Panels a and c illustrate the effects of IL *substitution* for NaI and *vice versa*, whereas panels c and d visualize the addition of either NaI or IL.

Figure 6a reveals that the substitution of EMImTFSI for NaI makes the anion I faster. By contrast, TFSI is distinctly slower in the 20/0.5/0.5 mixed-salt complex than in the pure PEO−IL complex 20/0/1. This will be closely connected to the 51 K difference in T_g between the two electrolytes (cf. Table 1). Moreover, in 20/0.5/0.5, the two anionic diffusivities do not differ much in magnitude. However, D^*_I exceeds D^*_{TFSI} at low T, while the reverse is true at high T, which involves a crossover temperature at about 130 °C. This may be due to the combination of two effects: ionic mobility and pair formation.

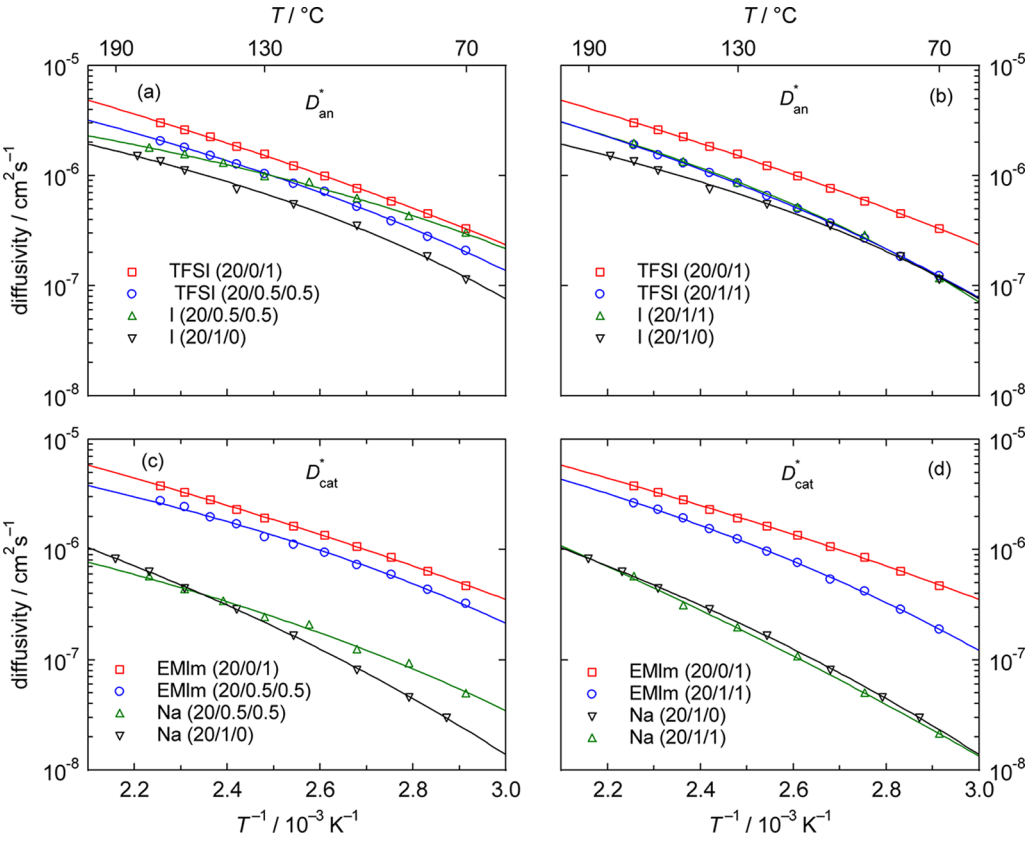

Figure 6. Diffusivity of cations ($D^*_{cat} = D^*_{Na}$ or D^*_{EMIm}) and anions ($D^*_{an} = D^*_I$ or D^*_{TFSI}) as a function of inverse temperature in single-salt and mixed-salt $PEO_{20}NaI_xEMImTFSI_y$ (20/x/y) electrolytes, as indicated, revealing the impact of salt substitution and salt addition: (a) NaI/IL substitution effects on D^*_{an}, (b) NaI/IL addition effects on D^*_{an}, (c) NaI/IL substitution effects on D^*_{cat}, (d) NaI/IL addition effects on D^*_{cat}. The solid lines are VTF fits serving to guide the eye.

dx.doi.org/10.1021/jp311563h | J. Phys. Chem. B 2013, 117, 2527−2534

On the basis of size and shape considerations, it seems plausible that I^- is more mobile than $TFSI^-$ within the same electrolyte.[15] However, the relatively small I^- ion is also more prone to neutral pair formation,[11] which relates to charge delocalization on the bulky $TFSI^-$ ion. Since ion pairing in SPEs *increases* with *increasing* temperature, and in addition, as pairs (predominantly NaI^0) move much slower than I^-,[7] the overall transport of iodine as expressed by D_I^* may fall below D_{TFSI}^* above a critical crossover temperature.

The influence of NaI/IL addition is depicted in Figure 6b. Compared to Figure 6a, the 20/0.5/0.5 data are replaced by 20/1/1 but those of the binary complexes are the same. It is seen that the data associated with the mixed-salt system take an intermediate position like in Figure 6a. However, both D_I^* and D_{TFSI}^* are smaller in 20/1/1 than 20/0.5/0.5 at the low end of the T range. It is remarkable that the diffusivities of I and TFSI virtually coincide despite their differences in size and structure. At the lowest temperatures, the addition of IL to 20/1/0 has no enhancing effect on D_I^*. Probably, these findings relate to the high total salt concentration in 20/1/1 leading to cooperative motion.

For cation substitution, Figure 6c shows a remarkable disparity between the magnitudes of D_{EMIm}^* and D_{Na}^*. Furthermore, the high EMIm diffusivity decreases by about 1/3 upon replacing half of the IL content by NaI. On the contrary, the low Na diffusivity increases due to the 50% replacement of NaI by IL over a wide range of lower temperatures. The strongest increase of slightly more than a factor of 2 appears at the lowest temperature investigated, whereas at high T even a decrease of D_{Na}^* is indicated by the data. The crossover between the two D_{Na}^* curves occurs near 150 °C. In this case, the observed behavior cannot be rationalized with ion pairing because very likely Na^+ and NaI^0 pairs have a similar mobility, as evidenced by modeling of ionic transport in PEO−NaI electrolytes[7] and molecular dynamics calculations.[16] Probably, the D_{Na}^* enhancement at lower T relates to the decrease of T_g by 25 K upon IL substitution (cf. Table 1; −37.6° for 20/0.5/0.5 versus −12.3° for 20/1/0). This enhancement may be reinforced by the 50% reduction of the Na concentration. To be specific, it was found that D_{Na}^* monotonically *increases* with *decreasing* salt concentration in binary PEO−NaI electrolytes.[7] Apparently, a less crowded occupation of the polymer chain by Na also contributes to the dynamics of this cation.

Figure 6d displays the impact of IL/NaI addition on cation diffusion. This panel shows the 20/1/1 data instead of the 20/0.5/0.5 data in panel c, while the binary complexes are naturally represented by the same data in both panels. Figure 6d reveals that adding NaI to the 20/0/1 complex causes a drop in D_{EMIm}^*. Going to lower temperature, this drop gets somewhat larger than in Figure 6c. However, adding IL to 20/1/0 has virtually no effect on D_{Na}^*. This indicates that the EO/Na ratio is the main parameter controlling D_{Na}^*, whereas the plasticizing effect of the ionic liquid seems to play only a minor role. Possibly the latter effect is counteracted by the increased ion density at this C_s level. A similar finding was made for D_I^* at lower T, as discussed above in connection with Figure 6b.

3.4. Ion Association. To quantify the impact of ion association, or more specifically ion pairing, one usually calculates the Nernst−Einstein deviation parameter Δ.[17] This so-called delta parameter is defined by the relationship $\sigma = \sigma_{diff}(1-\Delta)$, where σ_{diff} is the hypothetical overall conductivity derived from the joint individual contributions of all ionic diffusion coefficients obtained either by PFG-NMR or RTD.[17] Alternatively, one may write

$$\Delta = 1 - \frac{\sigma}{\sigma_{diff}} = 1 - \frac{D_\sigma}{D_{cat}^* + D_{an}^*} \quad (6)$$

where, in single-salt electrolytes, D_{cat}^* is either D_{EMIm}^* or D_{Na}^* and D_{an}^* is either D_{TFSI}^* or D_I^*. In the present 50%/50% mixed-salt cases, the mean cation and anion diffusivities enter eq 6, thus, e.g., $D_{cat}^* = (D_{EMIm}^* + D_{Na}^*)/2$. We note that the ratio σ/σ_{diff} appearing in eq 6 may be identified with the ionicity of the electrolyte.[18]

For the present electrolytes, Δ is plotted as a function of inverse temperature in Figure 7. It is seen that Δ is lowest for

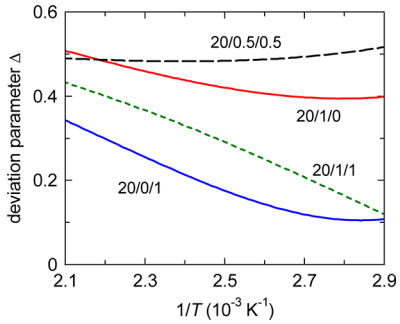

Figure 7. Nernst−Einstein deviation parameter Δ as a function of inverse temperature in single-salt and mixed-salt $PEO_{20}NaI_xEMImTFSI_y$ $(20/x/y)$ electrolytes, as indicated. The Δ data were calculated from the VTF fits in Figure 4 by using eq 6.

20/0/1, indicating that the bulky ions in this binary PEO-IL electrolyte do not promote pair formation. By contrast, the distinctly higher Δ values (0.4 to 0.5) for the pure PEO−NaI electrolyte 20/1/0 comply with the pronounced ion-pairing tendency found for this SPE system.[7] The large, virtually constant delta parameter ($\Delta \approx 0.5$) for the mixed-salt complex 20/0.5/0.5 seems surprising. However, our unpublished results on the PEO−EMImI system have shown that pairing between $EMIm^+$ and I^- is strong, as indicated by Δ values close to 0.6. Moreover, for PEO−NaI, it was found that the pair contribution increases with decreasing salt concentration, which may be rationalized by the strong interaction between Na and PEO and the concomitant role of the polymer conformational entropy.[7] Figure 7 further reveals that the more concentrated mixed-salt complex 20/1/1 takes an intermediate position. This is not easy to explain but may relate to the transition from a relatively dilute to a virtually concentrated electrolyte regime, in which cooperative effects are predominating.

4. DISCUSSION

Surveying the literature on polymer electrolytes, it has been established that small alkali-metal cations, such as Li and Na, form strong coordinative bonds with the oxygen atoms in the PEO chains.[19,20] As a result, the conformational freedom of the polymer is constrained, which is reflected by an increase of T_g. This situation leads to a strong correlation between the mobility of Li or Na and the motion of the polymer segments.[21] By contrast, the anions are not directly bound to the polymer, so that they commonly exhibit a higher diffusivity than the cations in classical SPE systems, such as PEO−NaI.[7,22,23]

dx.doi.org/10.1021/jp311563h | J. Phys. Chem. B 2013, 117, 2527−2534

In PEO−IL systems, however, the bulky organic cations only weakly coordinate to the polymer.[24,25] As a consequence, their diffusivity is high and may even exceed that of the anions, as found in this work for PEO_{20}EMImTFSI. This situation is reminiscent of pure ILs for which also $D^*_{cat} > D^*_{an}$ commonly holds.[26−28] Moreover, the ionic liquid may act as a plasticizer in the polymer matrix, thus reducing T_g of PEO (∼−60 °C), as confirmed by the T_g value obtained for PEO_{20}EMImTFSI in Table 1.

The present results show that many ion transport properties of the $PEO_{20}NaI_xEMImTFSI_y$ mixed-salt systems can be well interpreted within the conceptional framework described above. In particular, substitution of IL for NaI leads to acceleration of Na and I, whereas in the reverse case EMIm and TFSI get retarded. Similar effects are found for the addition of IL or NaI to the binary systems, however, with the exception that the Na diffusivity does not become faster (cf. Figure 6d) despite the IL-induced lowering of T_g. It should be emphasized, however, that the D^*_{Na} enhancement for IL-substitution (cf. Figure 6c) does not imply an improvement of the transport capacity $C_{Na}D^*_{Na}$, which seems crucial to potential sodium-battery performance. Rather, the twice as large Na diffusivity at lower T in 20/0.5/0.5 with respect to 20/1/0 is outweighed by the half as large Na concentration due to its 50% replacement by the IL cation.

Our findings may be compared with similar results obtained by Joost et al.[6] for $PEO_{20}LiTFSI_xPyr_{14}TFSI_y$ electrolytes with different concentrations of the inorganic salt LiTFSI and the ionic liquid Pyr_{14}TFSI, as specified by $x = 1$ or 2 and $y = 0$ to 4. These authors report an increase of the Li diffusivity by an IL addition that corresponds to the changeover from a 20/1/0 to a 20/1/1 composition. This increase amounts to about a factor of 1.5 at 50 °C. As indicated before, however, at this low temperature, the degree of crystallization may play a substantial role. In the same study, the partial replacement of Li by Pyr_{14}, thereby changing 20/2/0 to 20/1/1, resulted in a negligible D^*_{Li} increase. Altogether, these effects on D^*_{Li} are similar to the those on D^*_{Na} in the present work, although the C_s levels and the T ranges differ somewhat.

The above discussion and the evaluation of the diffusion data in section 3.3 are qualitative in nature and partly speculative. Some of the results are not well understood. This mostly applies to the finding that the Na diffusivity does not change upon IL addition to the 20/1/0 complex (cf. Figure 6d) despite the strong drop in T_g. Also the T dependence of the Na diffusion enhancement upon partially replacing NaI by IL (cf. Figure 6c) seems not easy to explain. Therefore, more detailed quantitative evaluations within ion transport models are necessary and currently in progress.

5. CONCLUSIONS

Summarizing the main results of this work, the following conclusions can be drawn: (1) The glass transition temperature of the mixed-salt-substituted and mixed-salt-added PEO−NaI/EMImTFSI polymer electrolytes are not much different and fall between the T_g values of the single-salt complexes (cf. Table 1). (2) Related to the T_g behavior, the D_σ vs $1/T$ curves of the mixed-salt electrolytes run close to each other and are centrally located between the corresponding curves for the single-salt complexes (cf. Figure 5). (3) *Substitution* of the ionic liquid EMImTFSI for NaI in PEO_{20}NaI by 50% leads to an *increase* of the iodine diffusivity over a wide T-range. Conversely, a similar substitution of NaI for IL in PEO_{20}EMImTFSI causes a *decrease* of the TFSI diffusivity (cf. Figure 6a). (4) Similar effects on anion diffusion are observed for the *addition* of IL/salt to the binary complexes. However, the influence on D^*_{TFSI} is larger than that on D^*_I, which even remains unaffected at low temperatures (cf. Figure 6b). (5) *Substitution* of IL for NaI in PEO_{20}NaI by 50% leads to an *increase* of the Na diffusivity at lower T by a factor of 2. Conversely, a similar substitution of NaI for IL in PEO_{20}EMImTFSI causes a *decrease* of the EMIm diffusivity (cf. Figure 6c). (6) The addition of IL to PEO_{20}NaI has virtually no effect on Na diffusion. By contrast, the addition of NaI to PEO_{20}EMImTFSI slows down the diffusion of EMIm (cf. Figure 6d). (7) The degree of ion association appears to be lowest in PEO_{20}EMImTFSI containing only IL as the salt component. No simple picture emerges from comparisons of the ion association parameter among all mixed-salt and single-salt complexes (cf. Figure 7).

A more general conclusion is that the inorganic cation (Na) in PEO-based amorphous electrolytes neither profits, in terms of transport capacity, from its partly substitution with IL nor from the addition of IL.

AUTHOR INFORMATION

Corresponding Author

*E-mail: stolwij@uni-muenster.de. Phone: +49 (0)251 8339013. Fax: +49 (0)251 8338346.

Notes

The authors declare no competing financial interest.

ACKNOWLEDGMENTS

We thank M. Wiencierz for making available his data on the PEO-NaI system as well as S. Lux and S. Passerini for providing ionic liquid of high purity. Financial support by the Deutsche Forschungsgemeinschaft is gratefully acknowledged.

REFERENCES

(1) Shin, J.-H.; Henderson, W. A.; Passerini, S. *Electrochem. Commun.* **2003**, *5*, 1060−1020.
(2) Shin, J.-H.; Henderson, W.; Appetecchi, G.; Alessandrini, F.; Passerini, S. *Electrochim. Acta* **2005**, *50*, 3859−3865.
(3) Appetecchi, G.; Kim, G.; Montanino, M.; Alessandrini, F.; Passerini, S. *J. Power Sources* **2011**, *196*, 6703−6709.
(4) Balducci, A.; et al. *J. Power Sources* **2011**, *196*, 9719−9730.
(5) Kim, Y. H.; Cheruvally, G.; Choi, J. W.; Ahn, J. H.; Kim, K. W.; Choi, D. S.; Song, C. E. *Macromol. Symp.* **2007**, *249−250*, 183−189.
(6) Joost, M.; Kunze, M.; Jeong, S.; Schönhoff, M.; Winter, M.; Passerini, S. *Electrochim. Acta* **2012**, *86*, 330−338.
(7) Wiencierz, M.; Stolwijk, N. A. *Solid State Ionics* **2012**, *212*, 88−99.
(8) According to the lot specifications, the PEO base material typically contained 1.4 wt % SiO_2 and 0.2 wt % CaO. These contaminations are inherent to the manufacturing process and present in the form of small particles.
(9) Obeidi, S.; Zazoum, B.; Stolwijk, N. *Solid State Ionics* **2004**, *173*, 77−82.
(10) Call, F.; Stolwijk, N. A. *J. Phys. Chem.Lett.* **2010**, *1*, 2088−2093.
(11) Stolwijk, N. A.; Wiencierz, M.; Heddier, C.; Kösters, J. *J. Phys. Chem. B* **2012**, *116*, 3065−3074.
(12) Tanner, J. E. *J. Chem. Phys.* **1970**, *52*, 2523−2526.
(13) Stolwijk, N.; Wiencierz, M.; Fögeling, J.; Bastek, J.; Obeidi, S. *Z. Phys. Chem.* **2010**, *224*, 1707−1733.
(14) With the definition of the charge diffusivity given in eq 5, D_σ should be smaller than the sum of the (mean) cation diffusivity D^*_{cat} and the (mean) anion diffusivity D^*_{an}. This condition is fulfilled for all investigated electrolytes. It relates to the fact that D_σ contains the salt concentration C_s instead of the total concentration of ion species, which equals $2C_s$.

(15) Tsuzuki, S. *ChemPhysChem* **2012**, *13*, 1664−1670.
(16) Maitra, A.; Heuer, A. *J. Phys. Chem. B* **2008**, *112*, 9641−9651.
(17) Boden, N.; Leng, S.; Ward, I. *Solid State Ionics* **1991**, *45*, 261−270.
(18) Tokuda, H.; Tsuzuki, S.; Susan, M. A. B. H.; Hayamizu, K.; Masayoshi, W. *J. Phys. Chem. B* **2006**, *110*, 19593−19600.
(19) Siqueira, L. J.; Ribeiro, M. C. *J. Chem. Phys.* **2005**, *122*, 194911.
(20) Borodin, O.; Smith, G. D. *Macromolecules* **2006**, *39*, 1620−1629.
(21) Kunze, M.; Karatas, Y.; Wiemhöfer, H.-D.; Schönhoff, M. *Macromolecules* **2012**, *45*, 8328−8335.
(22) Suarez, S.; Abbrent, S.; Greenbaum, S.; Shin, J.; Passerini, S. *Solid State Ionics* **2004**, *166*, 407−415.
(23) Diddens, D.; Heuer, A.; Borodin, O. *Macromolecules* **2010**, *43*, 2028−2036.
(24) Costa, L. T.; Ribeiro, M. C. *J. Chem. Phys.* **2006**, *124*, 184902.
(25) Eschen, T.; Kösters, J.; Schönhoff, M.; Stolwijk, N. A. *J. Phys. Chem. B* **2012**, *116*, 8290−8298.
(26) Noda, A.; Hayamizu, K.; Watanabe, M. *J. Phys. Chem. B* **2001**, *105*, 4603−4610.
(27) Stolwijk, N. A.; Obeidi, S. *Electrochim. Acta* **2009**, *54*, 1645.
(28) Hayamizu, K.; Tsuzuki, S.; Seki, S.; Umebayashi, Y. *J. Chem. Phys.* **2011**, *135*, 084505.